


Article

Design Optimisation for Cable Dome Structures Based on Progressive Collapse Resistance

Lian-Meng Chen ^{1,*}, Sun-Kai Yan ¹, Zhi-Chao Jiang ¹, Kai-Yu Huang ¹, Ze-Bin Li ¹, Wei Li ¹ , Yi-Yi Zhou ² and Shi-Lin Dong ³

¹ College of Civil Engineering and Architecture, Wenzhou University, Wenzhou 325035, China; yskjiayou666@163.com (S.-K.Y.); 17461572036@stu.wzu.edu.cn (Z.-C.J.); kive163202104@163.com (K.-Y.H.); 21461544038@stu.wzu.edu.cn (Z.-B.L.); liweiwoaini521@163.com (W.L.)

² College of Mechanics and Materials, Hohai University, Nanjing 210098, China; zhouyy@czu.cn

³ Space Structures Research Center, Zhejiang University, Hangzhou 310027, China; wzchenlm@sina.com

* Correspondence: 00151034@wzu.edu.cn; Tel.: +86-139-5779-0090

Abstract: This study proposed a framework of optimal design for flexible cable dome structures based on progressive collapse resistance. First, a quantitative evaluation method for nonlinear robustness based on robustness control theory to reflect the structural progressive collapse resistance was proposed. Second, an actual engineering structure was used as a case study to evaluate the effects of design parameters on structural robustness. Finally, a genetic algorithm was used as an optimisation algorithm to further optimise the element cross-section and the structural shape and obtain a combined optimisation rate. The results indicated that increasing the element cross-sectional area, decreasing the structural span, and increasing the rise-to-span ratio effectively improved the structural robustness. The structural robustness was also effectively improved through the optimal design of element cross-sections by increasing element cross-sections sensitive to structural robustness and decreasing those insensitive to structural robustness. In this study, the combined optimisation rate was 38.27%, which was not only greater than the individual optimisation rates of 11.2% for element cross-sectional area optimisation and 22.5% for structural shape optimisation but also the sum of these two rates.

Keywords: cable dome; flexible structures; structural robustness; parameter analysis; optimal design; genetic algorithm



Citation: Chen, L.-M.; Yan, S.-K.; Jiang, Z.-C.; Huang, K.-Y.; Li, Z.-B.; Li, W.; Zhou, Y.-Y.; Dong, S.-L. Design Optimisation for Cable Dome Structures Based on Progressive Collapse Resistance. *Buildings* **2023**, *13*, 2353. <https://doi.org/10.3390/buildings13092353>

Academic Editor: Hassan Karampour

Received: 15 August 2023

Revised: 11 September 2023

Accepted: 13 September 2023

Published: 15 September 2023



Copyright: © 2023 by the authors. Licensee MDPI, Basel, Switzerland. This article is an open access article distributed under the terms and conditions of the Creative Commons Attribution (CC BY) license (<https://creativecommons.org/licenses/by/4.0/>).

1. Introduction

Cable dome structures are flexible cable-strut tension structures based on Fuller's concept of tensegrity [1]. Because of their high cable strength and the ability to control their prestress distribution to optimise their stiffness, these structures offer advantages, such as a high crossing capacity, a light weight, a favourable shape, and a low cost, and have been widely used in practical engineering [2,3].

According to the literature, the optimal designs of large-span spatial structures mainly include a prestress optimisation design [4,5], an element cross-sectional area optimisation design [6], a structural shape optimisation design [7–9], and a structural topology optimisation design [9–11]. The majority of studies on prestress optimisation design have focused on minimising the prestress level, structure weight, strain energy, and support reaction forces. Similarly, many studies on element cross-sectional area optimisation and structural shape optimisation have focused on minimising the material weight and construction cost. However, in construction scenarios, the quantity of steel required is usually less than 30 kg·m^{−2}, and the weight of steel structures is usually low. Therefore, further studies on the optimisation of material weight may not add much value. Although studies on structural topology optimisation have mainly focused on spatial grid structures and other rigid spatial structure systems, such structural topology optimisation has not been fully

achieved in cable dome structures. As consumer demands become more complex, spatial structures are expected to involve larger spans, more complex forms, and more novel materials. Factors such as explosion impacts, extreme weather, and accidental damage have negative effects on structures. If high-strain bearing cables are damaged, the entire structure may progressively collapse [12–14]. Therefore, exploring the performance of structures, especially in terms of anti-progressive collapse and structural robustness, and optimising the design of cable dome structures in terms of progressive collapse resistance are key in structural engineering.

Different countries have different definitions of progressive structural collapse, but in general, progressive collapse can be regarded as a failure mode in which a local part of a structure is damaged, leading to the entire structure's failure or the collapse of the main structure [15,16]. The feature of the failure is that the structure is characterised by progressive, disproportionate, and severe damage caused by a small cause at the beginning. Therefore, it is significant to improve the ability of the structure to resist progressive collapse and disproportionate damage through reasonable design, that is, to enhance the robustness of the structure.

The concept of robustness was first proposed by mathematicians to solve the instability problem in optimisation in the 1960s [17] and was first applied to civil engineering after the progressive collapse of Ronan Point in London in 1968 [18]. Following the 9/11 terrorist attacks in the United States, which destroyed the World Trade Center, and the collapse of numerous buildings during the 2008 Wenchuan earthquake in China, global attention shifted toward the progressive collapse and robustness of buildings. However, according to the literature, the primary research objects of structural robustness have included frame structures [19], frame core tubes [20], bridges [21], and underground structures [22]. Although research has gradually expanded to include large-span structures, researchers have primarily focused on rigid spatial structures, such as trusses [23], grid frames [24], and latticed shells [25], and on rigid pretension structures, such as tension string structures [26] and chord-supported grid structures [27]. Nonetheless, a flexible cable dome differs from a rigid structure. Before prestress is applied, the structure is viewed as a mechanism. When active cables are tensioned, prestress is gradually generated, and the system starts exhibiting large deformations and rigid-body displacement. When the external load increases or when unexpected circumstances occur, such as an explosion, the structure likely starts exhibiting a nonlinear state, including defects resulting from element destruction or slack, and the structure turns into a mechanism. Thus, flexible cable dome structures are featured with strong nonlinearity characteristics, and conventional robustness evaluation methods for rigid structures are not applicable in the direct evaluation of robustness for the aforementioned cable dome structure.

In order to evaluate the robustness of the flexible cable dome structures and propose a framework of optimal design for this kind of flexible structure in terms of progressive collapse resistance, a novel robustness evaluation method for flexible cable dome structures was proposed, and an optimisation model based on structural robustness for this type of flexible structure was developed in this paper. First, a nonlinear robustness evaluation method for flexible cable dome structures was developed to reflect the structural progressive collapse resistance in Section 2, and the effects of design parameters, such as the element cross-section, structural span, and rise-to-span ratio, on structural robustness were analysed in Section 3. On this basis, on the condition that the structural quality should not be increased, the genetic algorithm was used to identify the optimal distribution of element section materials, the most appropriate structural shape, and the combined optimisation rate of element section material distribution and structural shape to increase the resistance of structures to disproportionate damage in Section 4. The results, as shown in Section 5, indicated that increasing the element cross-sectional area, decreasing the structural span, and increasing the rise-to-span ratio effectively improved the structural robustness. The structural robustness was also effectively improved through the optimal design of element cross-sections by increasing element cross-sections sensitive to structural robustness and

decreasing those insensitive to structural robustness. The combined optimisation rate of the element cross-sectional area and the structural shape was not only greater than the individual optimisation rate but also the sum of these two rates. Therefore, the proposed nonlinear robustness evaluation method, the laws of effects of various parameters on structural robustness, and the framework for optimal design in terms of the structural robustness of cable domes are of value to evaluate the structural robustness and improve the progressive collapse resistance of the flexible cable dome structures.

2. Fundamental Theory of Nonlinear Structural Robustness

For building structures, robustness is generally defined as the ability of a structure to withstand disproportionate damage [28]. Thus, the ratio of the output response to the input cause is usually calculated to evaluate the structural robustness of a building. Because of the nonlinear characteristics of cable domes, the relationship between the input cause and output response is related not only to the structural properties but also to the input causes, such as external loads. Therefore, the equation of motion of a structural system can be expressed as follows:

$$M\ddot{x}(t) + C\dot{x}(t) + Kx(t) = u(t) + w(t), \quad (1)$$

where M , C , and K are, respectively, the structural mass, damping, and stiffness matrices related to the input signals; $\ddot{x}(t)$, $\dot{x}(t)$, and $x(t)$ are the acceleration, velocity, and displacement vectors, respectively, and $u(t)$ and $w(t)$ are the nominal input vector and interference input vector in the time domain, respectively. To minimise the ratio of the output response to input interference and increase the structural resistance to disproportionate damage, H_∞ control theory is adopted, and the H_∞ norm of the transfer function $G(s)$ is minimised. The output vector generated by the input interference vector $w(t)$ is defined as $\Delta y(t)$, and the input interference $w(t)$ and interference output vector $\Delta y(t)$ are transformed into $W(s)$ and $\Delta Y(s)$, respectively, through the Laplace transformation. The transfer function $G_{w\Delta y}(s) \in H_\infty$, the input interference vector $W(s) \in H_2^m$, and the interference output vector $\Delta Y(s) \in H_2^n$ are then used. Subsequently, the L_2 performance criterion is introduced, and the infinite norm of the function matrix $G(s)$ is represented by an L_2 -induced norm as follows [29]:

$$I_R = \|G_{w\Delta y}(s)\|_\infty = \sup_{\|W\|_2 \neq 0} \frac{\|\Delta Y(s)\|_2}{\|W(s)\|_2}. \quad (2)$$

For the matrix space function $f, g \in L_2^n$, the inner product is defined as follows:

$$\langle f, g \rangle = \int_0^\infty f^T(t)g(t)dt. \quad (3)$$

Because $w(t)$ and $\Delta y(t) \in L_2$ are Laplace inverse transforms of $W(s)$ and $\Delta Y(s)$, according to the definition of the inner product and the Laplace inverse transformation, $W(s)$ and $\Delta Y(s)$ can be expressed as follows:

$$\|W(s)\|_2 = \|w(t)\|_2, \quad \|\Delta Y(s)\|_2 = \|\Delta y(t)\|_2. \quad (4)$$

By the substitution of Formula (4) into Formula (2), the robustness index of nonlinear structures can be expressed as follows:

$$I_R = \|G_{w\Delta y}(s)\|_\infty = \sup_{\|w\|_2 \neq 0} \frac{\|\Delta y(t)\|_2}{\|w(t)\|_2} \quad (5)$$

In the formula $\|(\cdot)\|_2 = (\int_0^\infty \|(\cdot)\|^2 dt)^{1/2} = (\int_0^\infty (\cdot)^T Q (\cdot) dt)^{1/2}$, Q is a weighed matrix. Because the evaluation index I_R reflects the sensitivity of structural robustness to

uncertain input interference, the smaller the evaluation index is, the higher the resistance of the structure is to uncertain input interference (i.e., the higher the structural robustness is).

If the structure is subjected to a conventional load F_0 and the external random interference load is $w(t)$, then the total load is $F = F_0 + w(t)$. If the external random interference load $w(t)$ obeys a normal distribution, then the total load F also obeys a normal distribution. According to the 3σ rule, the probability of interference occurrence reaches 99.74% in the interval $(\mu - 3\sigma, \mu + 3\sigma)$, and this interval is divided into m segments (which is taken as 100 in this study). The input disturbance and output response are defined as external uncertain disturbance load $w_k(t)$ and node displacement in this study. To calculate the nodal displacement vectors y_0 and y_k resulting from the conventional load F_0 and the total load F_k of conventional load and interference load, ANSYS 15.0 finite element software is used, which considers nonlinear characteristics such as stress stiffening, large displacement, and large deformation. The structural robustness index I_{Rk} in the k interval is then calculated as follows:

$$I_{Rk} = \frac{\|y_k - y_0\|_2}{\|w_k\|_2}, \quad k = 1, 2, 3, \dots, m/2, \quad (6)$$

where I_{Rk} is the sum of the two corresponding robustness indices under the total load generated by the conventional load and positive and negative interference loads, respectively, in the k interval. In all normal distribution intervals, the structural robustness index I_R is calculated as follows:

$$I_R = \sum_1^{m/2} Q(k) I_{Rk}, \quad (7)$$

where $Q(k)$ is the probability distribution function of the combined force of load F_k in the k interval and is used as a weighed coefficient in the interval. This function is calculated as follows:

$$Q(k) = \begin{cases} \int_{\frac{6k-3}{m}}^{\frac{6k+3}{m}} \frac{1}{\sqrt{2\pi}} e^{-t^2/2} dt, & k = 1 \sim \frac{m}{2} - 1 \\ 1 - \int_{-\infty}^{\frac{3-2k}{2}} \frac{1}{\sqrt{2\pi}} e^{-t^2/2} dt, & k = \frac{m}{2} \end{cases} \quad (8)$$

3. Case Study of Robust Parameter Analysis of a Cable Dome Structure

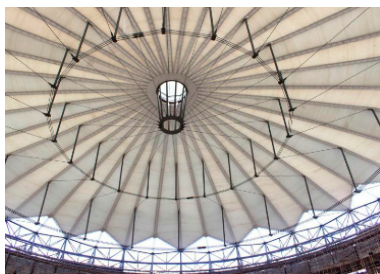
In this section, a Geiger-type cable dome used as the roof of the Inner Mongolia Yiqi National Fitness Sports Centre in China was considered in a case study. The diameter of the cable dome was 71.2 m, and its height was 5.5 m. Its structure was composed of 20 symmetrical cable-strut units and was supported by 20 surrounding hinge nodes. Each unit included tension cables and compression struts. The tension cables were divided into diagonal cables, ridge cables, and hoop cables. The diagonal cables were divided into diagonal cable 1 (DC1), diagonal cable 2 (DC2), and diagonal cable 3 (DC3). The ridge cables were divided into ridge cable 1 (RC1), ridge cable 2 (RC2), and ridge cable 3 (RC3). The hoop cables were divided into hoop cable 1 (HC1), hoop cable 2 (HC2), top hoop cable (THC), and lower hoop cable (LHC). The compression struts were divided into strut 1 (WG1), strut 2 (WG2), and strut 3 (WG3). For more details, please refer to Figure 1. Table 1 listed the cross-sectional areas, and initial prestress of the structure. In this study, robustness analysis was performed by using ANSYS software, in which the link180 element was used to simulate the cables and struts of the structure. The geometrical nonlinear effect of stress stiffening was also considered.

Table 1. Initial prestress and section parameters of the cable dome.

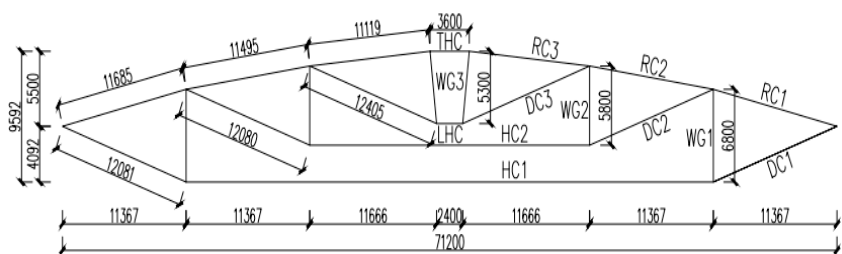
Element	Initial Prestress (kN)	Initial Area (m ²)	Optimal Design of Element Section		Combined Optimal Design	
			Optimisation Area (m ²)	Area Change Rate (%)	Optimisation Area (m ²)	Area Change Rate (%)
DC1	466.6	2.488×10^{-3}	2.787×10^{-3}	12.02	2.720×10^{-3}	9.32
DC2	208.0	8.53×10^{-4}	9.099×10^{-4}	6.67	7.734×10^{-4}	−9.33
DC3	105.9	6.05×10^{-4}	5.163×10^{-4}	−14.66	7.099×10^{-4}	17.34

Table 1. Cont.

Element	Initial Prestress (kN)	Initial Area (m ²)	Optimal Design of Element Section		Combined Optimal Design	
			Optimisation Area (m ²)	Area Change Rate (%)	Optimisation Area (m ²)	Area Change Rate (%)
RC1	682.2	1.844×10^{-3}	1.967×10^{-3}	6.67	1.623×10^{-3}	−11.98
RC2	473.1	1.361×10^{-3}	1.597×10^{-3}	17.34	1.452×10^{-3}	6.69
RC3	370.0	8.53×10^{-4}	1.001×10^{-3}	17.35	9.554×10^{-4}	12.00
WG1	−158.0	7.804×10^{-3}	6.451×10^{-3}	−17.34	6.243×10^{-3}	−20.00
WG2	−70.4	4.674×10^{-3}	3.864×10^{-3}	−17.33	4.487×10^{-3}	−4.00
WG3	−36.2	4.674×10^{-3}	3.864×10^{-3}	−17.33	3.988×10^{-3}	−14.68
HC1	1403.2	7.466×10^{-3}	8.163×10^{-3}	9.34	6.968×10^{-3}	−6.67
HC2	625.7	3.318×10^{-3}	3.805×10^{-3}	14.68	2.831×10^{-3}	−14.68
THC	1190.1	3.318×10^{-3}	3.539×10^{-3}	6.66	3.539×10^{-3}	6.66
LHC	305.3	3.318×10^{-3}	3.185×10^{-3}	−4.01	3.362×10^{-3}	1.33



(a) Structural model



(b) Structural profile

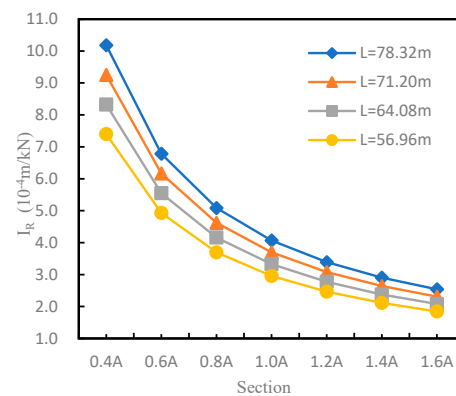
Figure 1. Cable dome structure of the Inner Mongolia Yiqi National Fitness Sports Centre.

3.1. Analysis of the Effects of Element Cross-Sectional Area and Structural Span on Structural Robustness

To analyse the effects of various element cross-sections and structural spans on structural robustness, section areas of all elements and structural spans were multiplied by several amplification values and reduction coefficients, and then robustness was calculated. The results are presented in Table 2 and Figure 2. First, at different structural spans, the robustness index considerably decreased with the increase of the element section (i.e., structural robustness was considerably enhanced). Compared with the original section, when the structural span was 71.20 m, and the element section decreased and increased 0.4 times, the structural robustness index increased and decreased by 66.8% and 28.6%, respectively. Second, when the structural span decreased, the structural robustness index decreased. In other words, when the section size of the element remained unchanged, the structure with the smaller span was more robust. Compared with the initial span of $L = 71.20$ m, when the section size remained unchanged, and the span decreased to $L = 64.08$ m and $L = 56.96$ m, the robustness index decreased by 10% and 20%, respectively. Third, as shown in Figure 2, when the element section increased, the slope of the curve, which indicates the relationship between structural robustness and the element section, gradually decreased, indicating that the structural robustness enhancement gradually decreased with the increase in the element section. Fourth, the calculations performed herein suggested that the changes in the element sections resulted in various levels of sensitivity to structural robustness. In this case, HC1 and RC3 were relatively sensitive, with DC1 and RC2 ranking second, and the effects of section changes of struts LHC and DC3 on structural robustness were negligible.

Table 2. Robustness indices with various element sections and structural spans (10^{-4} m/kN).

Span	0.4 A	0.6 A	0.8 A	1.0 A	1.2 A	1.4 A	1.6 A
$L = 78.32$ m	10.180	6.783	5.086	4.068	3.389	2.905	2.541
$L = 71.20$ m	9.252	6.165	4.622	3.697	3.081	2.640	2.310
$L = 64.08$ m	8.324	5.947	4.159	3.327	2.772	2.376	2.079
$L = 56.96$ m	7.397	4.980	3.696	2.957	2.464	2.112	1.847

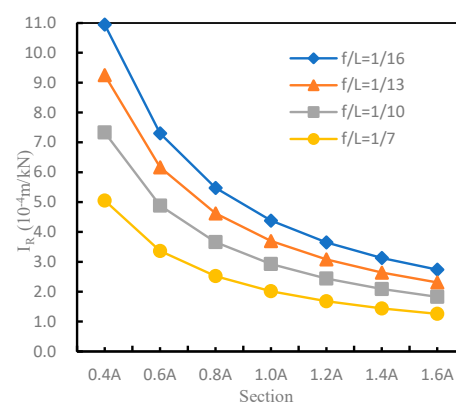
**Figure 2.** Robustness index with various cross sections and spans.

3.2. Analysis of the Effects of Rise-to-Span Ratio on Structural Robustness

To analyse the effects of the rise-to-span ratio on structural robustness, an initial span of $L = 71.20$ m was taken as an example of a constant structural span. As shown in Table 3 and Figure 3, at different element sections, the structural robustness indices were calculated at rise-to-span ratios (F/L) of $1/16$, $1/13$, $1/10$, and $1/7$. The results indicated that at the same element section, a larger rise-to-span ratio was associated with greater robustness. For example, in the original element section, when the rise-to-span ratio decreased from $1/13$ to $1/16$, the structural robustness index increased from 3.697×10^{-4} to 4.381×10^{-4} , an increase of 18.5%. However, when the rise-to-span ratio increased from $1/13$ to $1/10$ and $1/7$, the structural robustness index reached 2.927×10^{-4} and 2.016×10^{-4} , respectively, increases of 20.8% and 45.5%, respectively.

Table 3. Robustness indices with various element sections and rise-to-span ratios (10^{-4} m/kN).

Rise-to-Span Ratios	0.4 A	0.6 A	0.8 A	1.0 A	1.2 A	1.4 A	1.6 A
$f/L = 1/16$	10.947	7.301	5.477	4.381	3.651	3.130	2.738
$f/L = 1/13$	9.252	6.165	4.622	3.697	3.081	2.640	2.310
$f/L = 1/10$	7.334	4.884	3.660	2.927	2.439	2.090	1.829
$f/L = 1/7$	5.053	3.364	2.521	2.016	1.680	1.440	1.259

**Figure 3.** Robustness indices with various element sections and rise-to-span ratios.

4. Robustness-Based Optimal Design

Considering the effects of the various element sections and structural shapes on structural robustness, a genetic algorithm was used to identify the optimal distribution of the element section material and the structural shape depending on the robustness performance. The main code of the genetic algorithm was written in the numerical analysis software MATLAB 2018, and the structural modelling, node displacement value, and robustness index I_R were calculated in ANSYS. Subsequently, ANSYS was used along with MATLAB to crossread the data. The design process was detailed as follows.

- (1) The optimisation parameters were set in MATLAB, namely, the population size, encoding string length, crossover and mutation probability, and number of evolutionary iterations. The population size was set as 40, the encoding string length was set as 52, the crossover probability was set as 0.8, the mutation probability was set as 0.2, and the number of evolutionary iterations was set as 100. Subsequently, an optimisation variable was selected, and its actual value range was calculated. The initial population was then generated by binary coding.
- (2) The initial population generated by MATLAB was imported into ANSYS, and the structural robustness index I_R represented by each individual in the population was calculated. The number of the structural robustness indices was equal to the population size.
- (3) The structural robustness index I_R calculated by ANSYS was imported into MATLAB, and its reciprocal was used as a fitness function. Sequencing was then performed, and a replication, crossover, and mutation process was selected after the optimal individual was extracted from the initial population.
- (4) Steps 2 and 3 were repeated for cyclic iterative calculation, and the optimal individual from the offspring was extracted until optimal robustness was achieved. The process is depicted in Figure 4.

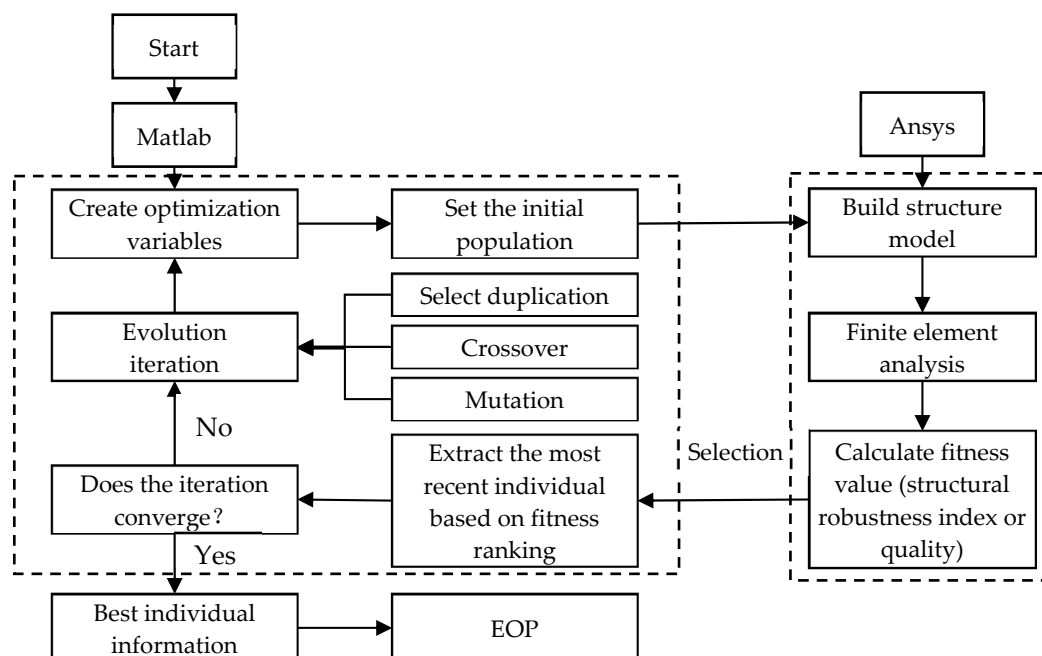


Figure 4. Flow chart of optimisation by the genetic algorithm.

4.1. Element Section Optimisation Design in Terms of Robustness

The section sizes of various elements were first selected as the optimisation variables, and the optimal section distribution of all types of elements within the sectional control scope was determined to obtain the minimum index of structural robustness, namely, the optimal robustness performance. The overall quality of the optimal structure M did not

exceed that of the initial structural model M_0 . The mathematical optimisation model was as follows:

$$\begin{cases} \min_A I_R = \|G(s)\|_2 \\ \text{s.t. } M \leq M_0 \\ A_{\min} \leq A_i \leq A_{\max} \end{cases} \quad (9)$$

where the control ranges of the element section areas were approximately 80% to 120% of the values of the initial structural model. Under the joint action of conventional and interference loads, the stress of all element types did not exceed the yield strength of the material. The overall quality of the initial structural model was $M_0 = 2138.96$ kg. Table 1 lists the section distributions of all elements after optimisation.

According to the optimisation results, when the number of iterations increased, the structural robustness index decreased before levelling off at the optimal target value of 3.282×10^{-4} m/kN. Compared with the initial structural model's robustness index of 3.697×10^{-4} m/kN, the optimisation rate was 11.2%. Following optimisation, the element sections of the cables either increased or decreased, and all the element sections of the struts decreased. The overall quality of the optimised structure M_0 was quantified at 2138.16 kg, which did not exceed the initial quality M . According to the degree of change of the element sections, the sections of HC1, RC3, DC1, and RC2, which were sensitive to structural robustness, increased. As for the struts and DC3, which were insensitive to structural robustness, the section reductions were considerable, with the sections of three types of struts decreasing by 17.34%, approaching the 20% limit value. Therefore, measures such as increasing the element sections that were sensitive to structural robustness and decreasing the element sections that were insensitive to structural robustness may effectively enhance the robustness performance of a structure.

4.2. Structural Shape Optimisation Design in Terms of Robustness

In this section, further investigation was conducted into the optimal design of structural shapes in terms of robustness. During the optimisation process, the overall form of the architecture remained unchanged. Therefore, the overall shape parameters, such as the number of symmetrical cable-strut units, the number of hoop cables, the rise-to-span ratio, and the elevation of the surrounding support nodes, remained unchanged as well. For safety, the structural shape parameters of the inner tension ring were not altered during shape optimisation. Thus, one symmetrical cable-strut unit was used as the research object during the optimisation of the structural shape, with three sets of shape parameters and six variables as the optimisation variables, namely, the top levels of struts, including top-level S1 of strut 1 and top-level S2 of strut 2; strut lengths, including length H1 of strut 1 and length H2 of strut2; and hoop cable radii, including radius R1 of HC1 and radius R2 of HC2 (Figure 5).

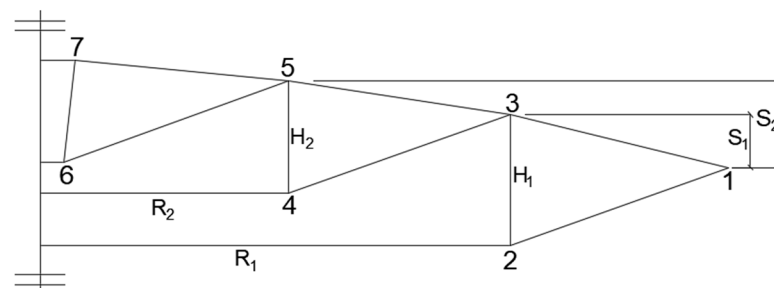


Figure 5. Shape parameters of a symmetrical cable-strut unit.

Similarly, the genetic algorithm was used to determine the optimal combination of three groups of optimisation variables within the control range in order to achieve optimal structural robustness. The optimal overall quality of the structure was also guaranteed not to exceed that of the initial structural model M_0 . The mathematical optimisation model of

the optimal overall quality was depicted in Formula (10), in which the control ranges of the optimisation variables S_i , H_i , and R_i were approximately 80% to 120% of the values of the initial structural model. The prestress of HC1 did not change during the structural shape optimisation process.

$$\begin{cases} \min_{S_i, H_i, R_i} I_R = \|G(s)\|_2 \\ M \leq M_0 \\ S_{imin} \leq S_i \leq S_{imax}, i = 1, 2 \\ H_{imin} \leq H_i \leq H_{imax} \\ R_{imin} \leq R_i \leq R_{imax} \end{cases} \quad (10)$$

Table 4 displays the optimised distributions of three groups of optimisation variables. When the number of iterations increased, the structural robustness index decreased until it plateaued at the optimal target value of 2.865×10^{-4} , with an optimisation rate of 22.50%, and the quality was 2137.44 kg, which satisfied $M \leq M_0$. Table 4 depicts the changes in the three groups of shape parameters following optimisation. The top level of strut 1 S_1 , the length of strut 2 H_2 , and the radius of the hoop cable R_1 were all considerably reduced, with change rates of -19.68% , -17.79% , and -16.54% , respectively, approaching the 20% limit value. The length of strut 1 H_1 and the radius of the hoop cable R_2 increased, with change rates of 9.29% and 4.25% , respectively. The top level of strut 2 S_2 remained unchanged. The shape optimisation results were also calculated under the condition that quality remained uncontrolled. Following optimisation, the robustness index I_R was 2.227×10^{-4} , with an optimisation rate of 39.8%, and the shape parameters for groups 1, 2, and 3 were $S_1 = 2.192$ and $S_2 = 3.813$, $H_1 = 8.139$ and $H_2 = 6.796$, and $R_1 = 22.516$ and $R_2 = 14.142$, respectively.

Table 4. Optimisation variables before and after structural shape optimisation.

Optimisation Variables	Initial Value (m)	Structural Shape Optimisation Design		Combined Optimal Design	
		Optimisation Value (m)	Change Rate (%)	Optimisation Value (m)	Change Rate (%)
S_1	2.708	2.175	-19.68	2.599	-4.03
S_2	4.418	4.439	0.48	3.888	-12.00
H_1	6.800	7.432	9.29	8.160	20.00
H_2	5.800	4.768	-17.79	6.496	12.00
R_1	24.233	20.226	-16.54	21.971	-9.33
R_2	12.866	13.413	4.25	13.038	1.34

4.3. Combined Optimal Design of Element Section and Structural Shape in Terms of Robustness

According to the element section optimisation design in Section 4.1 and the structural shape optimisation design in Section 4.2, the combined optimal design comprising the element section optimisation design and the structural shape optimisation design was further explored to determine the optimal combination of the three sets of shape optimisation variables and element section variables within the control range. The goal of the design was to achieve the minimum structural robustness index or the optimal robustness performance. During the shape optimisation process, the number of symmetrical cable-strut units, the number of hoop cables, and the rise-to-span ratio of the structure remained unchanged. Only three sets of shape parameters S_i , H_i , and R_i were considered as shape optimisation variables. Consequently, the optimisation variables of the combined optimal design were the sections of each element A_k and the three sets of shape parameters S_i , H_i , and R_i . During the optimisation process, the tension of HC1 remained unchanged, and the overall quality

of the optimised structure did not exceed that of the initial structural model M_0 . The mathematical optimisation model was represented as follows:

$$\begin{cases} \min_{S_i, H_i, R_i, A_k} I_R = \|G(s)\|_2 \\ M < M_0 \\ S_{imin} \leq S_i \leq S_{imax}, i = 1, 2 \\ H_{imin} \leq H_i \leq H_{imax}, i = 1, 2 \\ R_{imin} \leq R_i \leq R_{imax}, i = 1, 2 \\ A_{kmin} \leq A_k \leq A_{kmax}, k = 1, 2, \dots, 13 \end{cases} \quad (11)$$

where the control ranges of the optimisation variables S_i , H_i , R_i , and A_k were approximately 80% to 120% of the values of the initial structural model. The distribution of element sections and shape parameter changes following optimisation are depicted in Tables 1 and 4, respectively.

According to the optimisation results, when the number of iterations increased, the structural robustness index decreased until it plateaued at the optimal target value of 2.282×10^{-4} , with an optimisation rate of 38.27% compared with the initial structural robustness index of 3.697×10^{-4} . The effect was not only greater than the individual optimisation rates of 11.2% for element section optimisation and 22.5% for structural shape optimisation but also the sum of these two rates. This indicated that the combined optimisation of the element section and the structural shape may increase the mutual coupling effects between the two types of parameters. Following optimisation, the structural quality M was determined to be 2137.20 kg, satisfying the quality constraint condition $M < M_0$. After optimisation, various element sections displayed divergent trends. For instance, the sections of the ridge cables and diagonal cables either increased or decreased, the sections of the struts and hoop cables decreased, and the sections of the THC and LHC increased. These trends differed from those observed when the element section was individually optimised. During the optimisation process, the shape parameters also exhibited varying trends. The top level of the struts decreased, the length of the struts considerably increased, the radius of HC1 decreased, the radius of HC2 remained the same, and the variation of the length of strut 1 reached the limit value of 20%. These trends also differed from those obtained when the structural shape was individually optimised.

5. Conclusions

This study examined the quantitative evaluation method of nonlinear robustness for flexible cable domes and the framework for optimal design in terms of progressive collapse resistance and structural robustness. The main findings were as follows:

- (1) Structural robustness can be effectively improved by increasing the element section, decreasing the structural span, or increasing the rise-to-span ratio of the structure. It can also be effectively improved by optimising the element section and structural shape.
- (2) The optimal element section distribution, where the element sections that were sensitive to structural robustness were increased, and those that were insensitive to structural robustness were decreased, can improve structural resistance to disproportionate damage for a given level of structural quality.
- (3) Through the combined optimisation of the element section and the structural shape, robustness can be effectively improved with an optimisation rate of 38.27%. The optimisation rate of such optimisation was not only greater than the individual optimisation rates of 11.2% for element section optimisation and 22.5% for structural shape optimisation but also the sum of these two rates. These results suggested that the combined optimisation of the element section and the structural shape may enhance the coupling effects between the two types of parameters.

In addition, this paper mainly carried out element section optimisation and structural shape optimisation based on structural robustness. The next step can be topological optimisation so as to further improve structural robustness and progressive collapse resistance.

Author Contributions: Conceptualization, L.-M.C.; Methodology, L.-M.C., K.-Y.H. and Z.-B.L.; Software, S.-K.Y., Z.-C.J. and Z.-B.L.; Validation, Z.-C.J. and K.-Y.H.; Resources, L.-M.C., W.L., Y.-Y.Z. and S.-L.D.; Writing – original draft, L.-M.C.; Writing – review & editing, L.-M.C. and S.-K.Y.; Supervision, W.L., Y.-Y.Z. and S.-L.D.; Project administration, L.-M.C. All authors have read and agreed to the published version of the manuscript.

Funding: This research was funded by National Natural Science Foundation of China, grant number 51578422 and 51678082.

Acknowledgments: This research was supported by the National Natural Science Foundation of China (Grant nos. 51578422 and 51678082).

Conflicts of Interest: The authors declare no conflict of interest.

References

- Fuller, R.B. Tensile-Integrity Structures. U.S. Patent 3063521, 13 November 1962.
- Geiger, D.H. The design and construction of two cable domes for the Korean Olympics Shells, Membranes and Space Frames, Proceedings. *IASS Symp.* **1986**, *2*, 265–272.
- Levy, M.P. The Georgia dome and beyond achieving light weight-long span structures. In *Spatial, Lattice and Tension Structures: Proceedings of the IASS-ASCE International Symposium 1994; Held in Conjunction with the ASCE Structures Congress XII, Atlanta, GA, USA, 24–28 April 1994*; Amer Society of Civil Engineers: Atlanta, GA, USA, 1994; pp. 560–562, ISBN 0-87262-953-8.
- Quagliaroli, M.; Malerba, P.G.; Albertin, A.; Pollini, N. The role of prestress and its optimization in cable domes design. *Comput. Struct.* **2015**, *161*, 17–30. [[CrossRef](#)]
- Chen, L.-M.; Dong, S.-L. Optimal prestress design and construction technique of cable-strut tension structures with multioverall selfstress modes. *Adv. Struct. Eng.* **2013**, *16*, 1633–1644. [[CrossRef](#)]
- Yuan, X.-F. Optimal design of cable domes. *Spat. Struct.* **2002**, *8*, 51–56. [[CrossRef](#)]
- Liang, X.-T.; Yuan, X.-F.; Li, A.-L. Multi-objective shape optimization design of cable dome. *J. Huazhong Univ. Sci. Technol. (Nat. Sci. Ed.)* **2016**, *44*, 110–115. [[CrossRef](#)]
- Upadhyay, B.D.; Sonigra, S.S.; Daxini, S.D. Numerical analysis perspective in structural shape optimization: A review post 2000. *Adv. Eng. Softw.* **2021**, *155*, 102992. [[CrossRef](#)]
- Ma, T.; Zhao, X.-Z.; Gao, B.-Q. Combined shape and topology optimization of free-form structure. *J. Zhejiang Univ. (Eng. Sci.)* **2015**, *49*, 1946–1951. [[CrossRef](#)]
- Zuo, Z.-H.; Xie, Y.-M. Evolutionary topology optimization of continuum structures with a global displacement control. *Comput.-Aided Des.* **2014**, *56*, 58–67. [[CrossRef](#)]
- Rad, M.M.; Habashneh, M.; Logo, J. Reliability based bi-directional evolutionary topology optimization of geometric and material nonlinear analysis with imperfections. *Comput. Struct.* **2023**, *287*, 107120. [[CrossRef](#)]
- Martin, R.; Delatte, N. Another Look at Hartford Civic Center Coliseum Collapse. *J. Perform. Constr. Facil.* **2001**, *15*, 31–36. [[CrossRef](#)]
- Starossek, U. Progressive collapse of structures: Nomenclature and procedures. *Struct. Eng. Int.* **2006**, *16*, 113–117. [[CrossRef](#)]
- Chiang, J.C. Quality engineering design and construction in malaysia: A fast disappearing and endangered commodity. *Pap. Ser. Struct. Eurocodes* **2010**, *12*, 34–36.
- Wolff, M.; Starossek, U. Cable loss and progressive collapse in cable-stayed bridges. *Bridge Struct.* **2009**, *5*, 17–28. [[CrossRef](#)]
- Song, B.I.; Sezen, H. Experimental and analytical progressive collapse assessment of a steel frame building. *Eng. Struct.* **2013**, *56*, 554–672. [[CrossRef](#)]
- Huber, P.J.; Ronchetti, E.M. *Robust Statistics*; Wiley: New York, NY, USA, 2009.
- Person, C.; Delatte, N. Ronan point apartment tower collapse and its effect on building codes. *J. Perform. Constr. Facil.* **2005**, *19*, 172–177. [[CrossRef](#)]
- Masoero, E.; Wittel, F.K.; Herrmann, H.J.; Chiaia, B.M. Hierarchical structures for a robustness-oriented capacity design. *J. Eng. Mech.* **2012**, *138*, 1339–1347. [[CrossRef](#)]
- Noldgen, M.; Fehling, E.; Riedel, W.; Thoma, K. Vulnerability and robustness of a security skyscraper subjected to aircraft impact. *Comput.-Aided Civ. Infrastruct. Eng.* **2012**, *27*, 358–368. [[CrossRef](#)]
- Yan, D.; Chang, C.C. Vulnerability assessment of single-pylon cable-stayed bridges using plastic limit analysis. *Eng. Struct.* **2010**, *32*, 2049–2056. [[CrossRef](#)]
- Gao, Y. Quantitative analysis of structural robustness and its application in underground frame structures. *J. Build. Struct.* **2018**, *39*, 153–161. [[CrossRef](#)]

23. Richardson, J.N.; Coelho, R.F.; Adriaenssens, S. Robust topology optimization of truss structures with random loading and material properties: A multiobjective perspective. *Comput. Struct.* **2015**, *154*, 41–47. [\[CrossRef\]](#)
24. Zhu, J.-J. Topology Optimization and Robustness Analysis of Space Grid Structure. Master's Thesis, Zhejiang University, Hangzhou, China, 2016.
25. Wu, C.-B.; Gao, B.-Q. Lifecycle-cost analysis for reticular shells based on nonlinear robustness. *Spat. Struct.* **2018**, *24*, 11–15+22. [\[CrossRef\]](#)
26. Ye, J.; Gao, B.-Q.; Dong, S.-L. Linear robustness based optimization design of cable supported structure and its performance analysis. *Chin. J. Comput. Mech.* **2014**, *31*, 149–154. [\[CrossRef\]](#)
27. Shan, Y.-L.; Ye, J.; Gao, B.-Q. Robust configuration analysis and experimental study of cable supported hyperbolic flat latticed shell structure. *J. Build. Struct.* **2013**, *34*, 50–56. [\[CrossRef\]](#)
28. Starossek, U.; Haberland, M. Disproportionate collapse: Terminology and procedures. *J. Perform. Constr. Facil.* **2010**, *24*, 519–528. [\[CrossRef\]](#)
29. Mei, S.-W.; Sheng, T.-L.; Liu, K.-Z. *Modern Robust Control Theory and Application*; Tsinghua University Press: Beijing, China, 2008; Volume 61–63, pp. 142–143. (In Chinese)

Disclaimer/Publisher's Note: The statements, opinions and data contained in all publications are solely those of the individual author(s) and contributor(s) and not of MDPI and/or the editor(s). MDPI and/or the editor(s) disclaim responsibility for any injury to people or property resulting from any ideas, methods, instructions or products referred to in the content.